Journal of the Physical Society of Japan
Vol. 78, No. 5, May, 2009, 054709

Trimer V^{3+} Spin Singlet State and Pseudo Gap in $LiVS_2$ Studied by ^{51}V and ^{7}Li Nuclear Magnetic Resonance

Tetsu TANAKA, Yu KAWASAKI*, Shigeki ENDOU, Satoshi KIMURA, Yukiichi IDETA, Yutaka KISHIMOTO, Takashi OHNO, Naoyuki KATAYAMA[1,2], Minoru NOHARA[1,2], and Hidenori TAKAGI[1,2,3]

Department of Quantum Materials Science, University of Tokushima, Tokushima 770-8506
[1]*Department of Advanced Materials Science, University of Tokyo, Kashiwa, Chiba 277-8561*
[2]*CREST, Japan Science and Technology Agency*
[3]*The Institute of Physical and Chemical Research (RIKEN), Wako, Saitama 351-0198*

(Received November 27, 2008; accepted February 20, 2009; published April 27, 2009)

To clarify the electronic state in a two-dimensional triangular lattice $LiVS_2$, we have performed ^{51}V- and ^{7}Li-NMR measurements. Below the phase transition temperature T_c of about 310 K from the paramagnetic state to a nonmagnetic state, the Knight shift of both ^{51}V and ^{7}Li does not depend on temperature. The ^{51}V and ^{7}Li spin–lattice relaxation rates $1/T_1$ show the exponential temperature dependence below T_c, which indicates a gap structure of the electronic state. These results are in agreement with a trimer singlet of V^{3+} spins below T_c. The increase in ^{7}Li $1/T_1$ above T_c indicates the existence of the pseudo gap and agrees with the increase in paramagnetic susceptibility with increasing temperature and with the small entropy change at T_c compared with that in $LiVO_2$.

KEYWORDS: $LiVS_2$, two-dimensional triangular lattice, trimer spin singlet, Knight shift, spin–lattice relaxation
DOI: 10.1143/JPSJ.78.054709

1. Introduction

The novel critical phenomenon appearing near the Mott critical point is one of the most important topics in solid state physics. When geometrical frustration is added to a typical Mott insulator system, the antiferromagnetic insulator phase becomes unstable and an ambiguous ground state (for example, spin singlet state and spin liquid) appears. The electromagnetic properties of a two-dimensional triangular lattice (so-called spin frustration system) have received new attention. In a two-dimensional antiferromagnetic $S = 1/2$ Heisenberg triangular lattice, two spins can be antiparallel, but the third spin cannot be antiparallel to both of the former two spins; thus, they are oriented 120° to each other at the ground state without long-range ferromagnetic or antiferromagnetic ordering. Na_xCoO_2 has a triangular lattice and becomes a superconductor when an appropriate quantity of H_2O is added into an interlayer,[1] where the superconducting phase appears close to the magnetic phase. It may be considered that $LiVS_2$ would become a superconductor when, for example, H_2O or a certain molecule is added. Cooper pairing might be caused by the spin frustration when we could weaken the spin gap and develop the metallic phase.

Rudorff *et al.*, Imai *et al.*, Tian *et al.*, Onoda *et al.*, and Pen *et al.* have studied the phase transition and spin dynamics of a triangular lattice $LiVO_2$.[2–4] Its magnetic susceptibility is nearly constant below the phase transition temperature T_c of ~500 K from the nonmagnetic state to the paramagnetic state, abruptly increases at T_c, and decreases slowly obeying the Curie–Weiss law above T_c with increasing temperature. The electrical resistivity also decreases suddenly at T_c. Superlattice diffractions have also been observed below T_c. From these results, Goodenough and coworkers have suggested a singlet state of triangular clusters of V^{3+}–V^{3+}–V^{3+} bonded ions, that is, a trimer.[5,6]

Since van Laar and Ijdo synthesized $LiVS_2$,[7] the interesting physical properties of Li_xVS_2 $(0 \leq x \leq 1)$ (for example, metal–insulator transition and spin singlet insulator transition) have been reported.[8] $LiVS_2$ could also be a good candidate for the study of a spin system with a two-dimensional triangular lattice. Above the phase transition temperature T_c of about 310 K, the magnetic susceptibility χ of $LiVS_2$ decreases slowly with decreasing temperature but suddenly decreases below T_c as if it were nonmagnetic.[8] With decreasing temperature, the conductivity σ of $LiVS_2$ increases very slowly above T_c (metallic behavior) but decreases suddenly and approaches a value of two orders of magnitude smaller below T_c. These abrupt decreases in χ and σ indicate that a spin singlet V^{3+} trimer is being formed, that is, $LiVS_2$ is paramagnetic at high temperatures and becomes nonmagnetic below $T_c \sim 310$ K by the trimerization of V^{3+} spins, as discussed in $LiVO_2$.[3,4] As reported in $LiVO_2$, the superlattice structure has also been observed below the phase transition temperature T_c.[8] To investigate the electronic state of $LiVS_2$ from a microscopic point of view, we have performed ^{51}V- and ^{7}Li-NMR spectral analysis, and spin–lattice relaxation rate measurements.

2. Experimental

The powder sample has been synthesized by solid state reaction. The detailed preparation method for $LiVS_2$ is reported elsewhere.[8] The synthesized sample has been examined crystallographically with an X-ray diffractometer and magnetically with a superconducting quantum interference device (SQUID) magnetometer and electrical resistivity measurements. The obtained data agree with those reported previously.[9] The hysteretic behavior of the temperature dependence of χ shows that the transition from the nonmagnetic state to the magnetic state is of the first order and occurs at 303–316 K during heating and at 300–312 K during cooling. From the middle of each temperature range of the transition, $T_c = 310$ K and $T_c' = 306$ K are defined.

*E-mail: yu@pm.tokushima-u.ac.jp

We enclose the powder sample in a capsule made of Stycast 1266 (Emerson & Cuming) with a heat exchanger He gas to prevent a possible degeneration of the sample in the atmosphere. When the sample is cooled across the phase transition temperature, we change the temperature of the sample at a rate lower than -2 K/min to avoid a probable disorder of Li^+ ions.

The ^{51}V- and ^{7}Li-NMR measurements have been performed at temperatures between 4.2 and 470 K by employing a laboratory-built phase-coherent pulsed NMR spectrometer. We have measured the NMR spectrum by tracing the integrated spin–echo signal as a function of an external magnetic field using a box-car integrator. The ^{7}Li-NMR spectra above 340 K are obtained by the Fourier transformation of the spin echo. The nuclear spin–lattice relaxation rate $1/T_1$ has been obtained by measuring the recovered longitudinal nuclear magnetization $M(t)$ at the time t after a saturating pulse. The predicted functional expression for $M(t)$ for ^{51}V nuclei with $I = 7/2$ is the sum of four exponential terms,

$$\frac{M(\infty) - M(t)}{M(\infty)} = 0.019\exp\left(-\frac{t}{T_1}\right) + 0.0682\exp\left(-\frac{6t}{T_1}\right) + 0.206\exp\left(-\frac{15t}{T_1}\right) + 0.714\exp\left(-\frac{28t}{T_1}\right), \quad (1)$$

where the coefficients have been obtained by theoretical calculation for the transition between $I_z = -1/2$ and $+1/2$ spin levels.[10] The fitting of $M(t)$ to the measured data points is good and gives $1/T_1$ at each temperature. The observed recovery of ^{7}Li longitudinal nuclear magnetization is single exponential and the relaxation rate $1/T_1$ is well defined in the entire measured temperature range.

3. Results and Discussion

We show the ^{51}V-NMR spectrum measured at 15.25326 MHz at 77.3 K in Fig. 1. The spectrum shows resonance peaks at 1.298, 1.316, 1.333, 1.354, 1.358, 1.373, 1.394, and 1.408 T in the polycrystalline sample, which is the so-called powder pattern for nuclei with $I = 7/2$. Here, the splitting (36 G) of the central line into two lines is induced by a second-order perturbation of the nuclear quadrupole interaction added to the Zeeman interaction. We estimate the quadrupole coupling constant ν_Q to be 0.42 MHz from the distance between the satellite lines, which is comparable to 0.47 MHz for $LiVO_2$. The asymmetric parameter $\eta = (V_{xx} - V_{yy})/V_{zz}$ in $LiVS_2$ is estimated to be 0.11 and is much smaller than $\eta = 0.40$ in $LiVO_2$.[3,11] The electric field gradients at ^{51}V nuclei in $LiVS_2$ are more symmetric than those in $LiVO_2$. This is consistent with the fact that the NMR spectra in $LiVO_2$ are broader than those in $LiVS_2$.[11]

The ^{51}V-NMR spectra have been measured at a higher magnetic field to gain a higher signal-to-noise ratio. The ^{51}V-NMR spectra measured at the fixed frequency of 129.1 MHz at several temperatures are shown in Fig. 2. We should note that $LiVS_2$ shows hysteretic behavior in the temperature dependence of both χ and σ,[8,9] which indicates that this phase transition is of the first order. We have measured all the present NMR spectra at a fixed temperature after the temperature is increased from its lowest value.

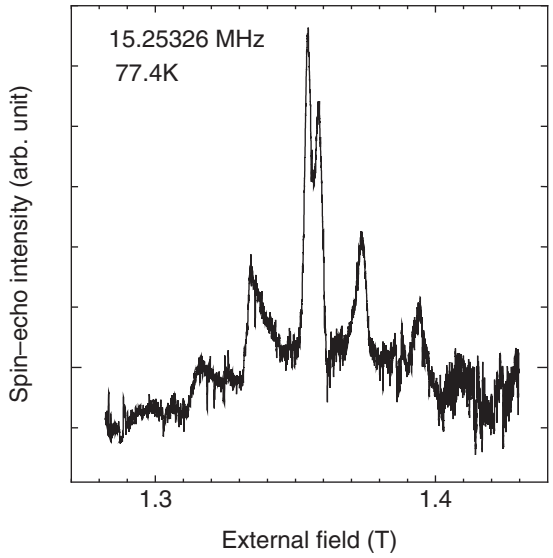

Fig. 1. ^{51}V-NMR spectrum at 15.25326 MHz and 77 K.

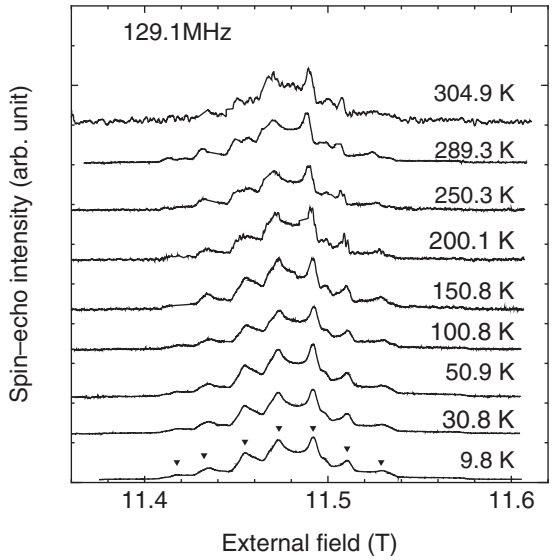

Fig. 2. ^{51}V-NMR spectra of $LiVS_2$ measured at 129.1 MHz at several temperatures.

We have observed seven split peaks in the ^{51}V-NMR spectra, where each peak is indicated by a triangle for 9.8 K, as shown in Fig. 2.[12] The splitting of the central line is not clear in these spectra. The width of the line increases because of the small splitting of this line, which is expected to be about 5 G for this experimental condition. We estimate the quadrupolar coupling constant ν_Q to be 0.42 MHz, which is in agreement with that estimated from the spectra observed at a low magnetic field. ν_Q does not depend on temperature over the measured temperature range between 9.8 and 305 K within the sensitivity of our apparatus, indicating that the lattice around V is not markedly changed by temperature below T_c. No spectrum can be observed above $T_c = 310$ K because its intensity decreases rapidly, which may be due to the decrease in spin–spin relaxation time T_2, as shown in the inset figure in Fig. 4, and the increase in line width due to the phase transition from the nonmagnetic insulating state to the paramagnetic metallic state. We have carefully searched for the spectrum that

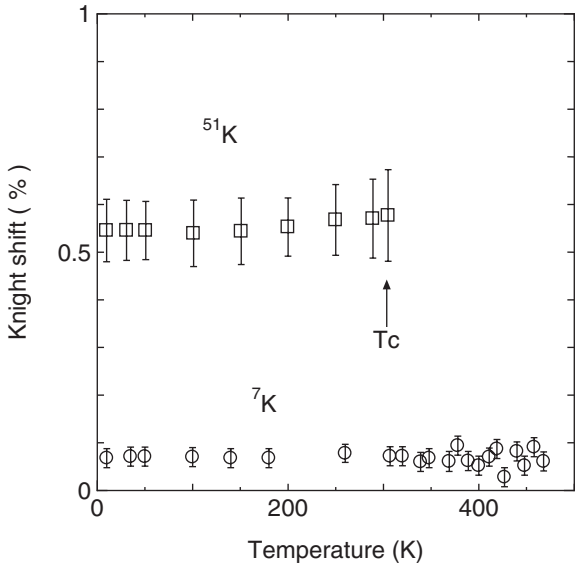

Fig. 3. Temperature dependence of Knight shift ^{51}K (squares) and ^{7}K (circles) measured at 129.1 MHz in $LiVS_2$. Error bars represent the corresponding FWHM values of the ^{51}V- and ^{7}Li-NMR spectra.

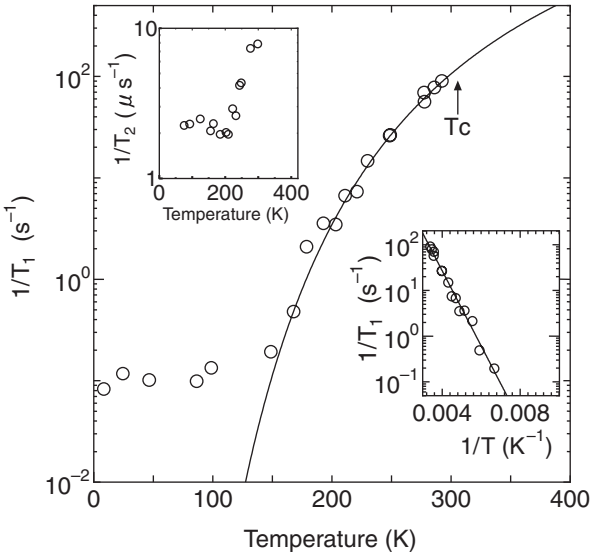

Fig. 4. Temperature dependence of ^{51}V nuclear spin–lattice relaxation rate $1/T_1$ measured in $LiVS_2$. The solid curve represents the fitting of an activation-type curve to the data points between 150 and 300 K, giving an energy gap of ~1900 K. The temperature dependence of $1/T_2$ is shown in the inset in the upper left.

shifted to another resonance field owing to paramagnetism above T_c, but we cannot find the signal.

We show the temperature dependence of the Knight shift ^{51}K estimated from the resonance magnetic field of the ^{51}V-NMR central line by squares in Fig. 3. Error bars indicate the corresponding full width at half maximum (FWHM) in the ^{51}V-NMR spectra. $^{51}K \sim 0.55\%$ does not depend on temperature in the measured temperature range below T_c. This temperature-independent Knight shift provides evidence for the nonmagnetic state below T_c. Since V^{3+} spins vanish because of a trimer singlet state below T_c,[8] the positive value of ^{51}K indicates that a core-polarization interaction is not dominant for the hyperfine field at ^{51}V site in $LiVS_2$, which is consistent with the discussion which will be given below on the observed temperature dependence of $1/T_1$. These results indicate that $LiVS_2$ is nonmagnetic below T_c and that ^{51}K and χ mainly originate from the Van Vleck orbital angular momentum.

The constant value of $^{51}K \sim 0.55\%$ below T_c is comparable to that reported in $LiVO_2$.[3] In contrast, the value of χ below T_c in $LiVS_2$ is twice as large as that in $LiVO_2$.[3,8] Generally, the Knight shift K_{orb} coming from the orbital contribution is given by $K_{orb} = 2\chi_{orb}\langle 1/r^3\rangle$, where χ_{orb} is an orbital component of χ and $\langle 1/r^3\rangle$ is the expectation value of $1/r^3$ over the 3*d*-wave function. $\langle 1/r^3\rangle$ for the V ion in $LiVS_2$ is about one-half that in $LiVO_2$, and the 3*d*-wave function of the V ion spreads over a wider area in $LiVS_2$ than in $LiVO_2$, which is consistent with the following point. The lattice constant *a*, the distance between the V^{3+} ions in $LiVS_2$, is larger than *a* in $LiVO_2$, and *c*, the distance between the V^{3+} ion plane and the S^{2-} ion plane in $LiVS_2$, is smaller than *c* in $LiVO_2$.[3,8] By considering these situations, it is suggested that the covalent coupling between V^{3+} and S^{2-} ions in $LiVS_2$ is stronger than that between V^{3+} and O^{2-} ions in $LiVO_2$, and the degree of two-dimensionality in $LiVS_2$ might be lower than that in $LiVO_2$.

Next, we report the nuclear spin–lattice relaxation rate $1/T_1$. The measured recovery of ^{51}V nuclear magnetization $M(t)$ after the saturating pulse is well fitted to eq. (1) given in §2 and gives $1/T_1$ at each temperature.[12] Figure 4 shows the temperature dependence of the obtained ^{51}V $1/T_1$. $1/T_1$ is nearly constant below ~100 K and increases exponentially with increasing temperature up to $T_c \sim 310$ K. The temperature dependence of $1/T_1$ in $LiVS_2$ resembles that in $LiVO_2$,[3] which suggests that the electronic states of these compounds are similar below T_c. This exponential behavior indicates that the spin excitation mode or the electronic density of states has an energy gap Δ and $1/T_1$ varies following

$$1/T_1 \propto \exp(-\Delta/k_B T), \tag{2}$$

where k_B is the Boltzmann constant. The solid curve in Fig. 4 shows the best fitted curve of eq. (2) to the data points between 150 and 300 K, and the energy gap Δ is estimated to be about 1900 K. The inset in Fig. 4 shows the Arrhenius plot of $1/T_1$ against $1/T$ between 150 and 300 K. This activation-type temperature dependence of $1/T_1$ indicates that the thermally excited V^{3+} spins over this energy gap yield a temperature-independent spin–lattice relaxation.

On the other hand, the observed Knight shift ^{51}K is independent of temperature, as discussed above. Thermally excited V^{3+} spins do not contribute to ^{51}K, which means that the hyperfine field and the core polarization at ^{51}V nuclei due to thermally excited V^{3+} spins are very small compared with the hyperfine field due to the orbital moment. This estimated energy gap 1900 K is comparable to but slightly larger than the gap 1600 K observed in $LiVO_2$.[3] The energy gap ~1600 K reported in $LiVO_2$ seems to be very small when it is compared with ~1900 K in $LiVS_2$, because $T_c \sim 500$ K in $LiVO_2$ is higher than $T_c \sim 310$ K in $LiVS_2$.

The nearly constant behavior of $1/T_1$ below 100 K may be caused by independent fluctuations of the paramagnetic impurity V spins observed as a Curie tail in χ at low temperatures.[8] The existence of this energy gap 1900 K provides evidence for the formation of the trimer spin singlet

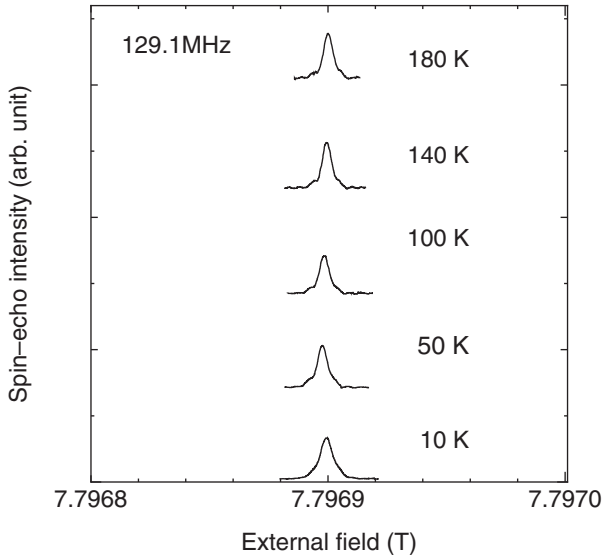

Fig. 5. ^{7}Li-NMR spectra of $LiVS_2$ measured at 129.1 MHz at several temperatures.

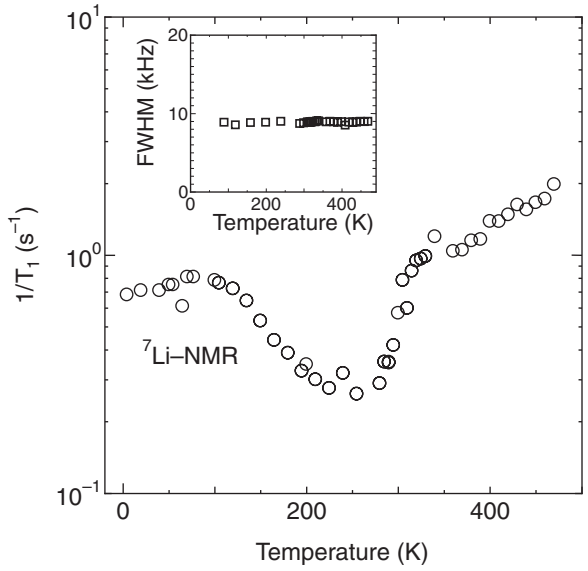

Fig. 6. Temperature dependence of ^{7}Li nuclear spin–lattice relaxation rate $1/T_1$ measured in $LiVS_2$. The temperature dependence of FWHM of the ^{7}Li-NMR spectra in $LiVS_2$ is also shown in the inset.

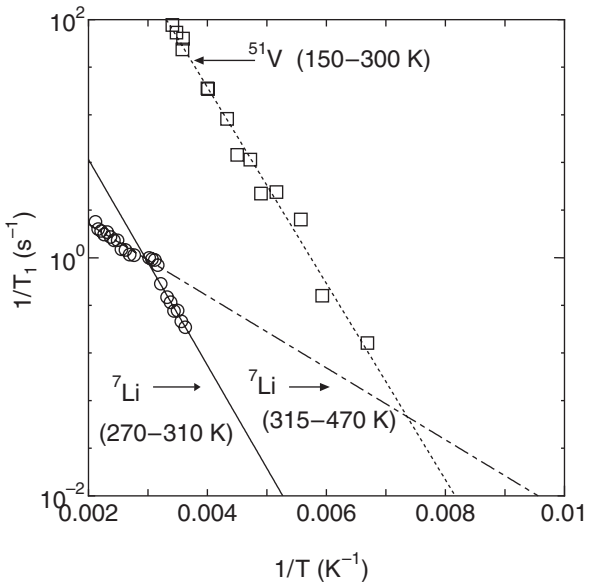

Fig. 7. Arrhenius plots of $1/T_1$ values of ^{51}V (squares, 150–300 K) and ^{7}Li (circles, 270–310 and 315–470 K) against $1/T$.

state in $LiVS_2$. This trimer spin singlet state is also supported by the superlattice observed in the electron diffraction.[8] A honeycomb-type diffuse streak is observed by electron diffraction in a metallic phase in $LiVS_2$. This diffuse streak becomes weak just above T_c, and therefore, this diffuse streak does not come from the thermal vibration or lattice defect, and it can be due to the development of the long-range ordering for V^{3+} spin trimerization.

We have also measured ^{7}Li-NMR. Figure 5 shows the ^{7}Li-NMR spectra at several temperatures. Their FWHM is $\sim$22 G and very small. Each ^{7}Li-NMR spectrum is considered to be composed of the overlapped central and two satellite lines because the quadrupole interaction is generally small for ^{7}Li. The ^{7}Li Knight shift ^7K is determined from the peak resonance field at each temperature. The circles in Fig. 3 show the temperature dependence of ^7K. $^7K = 0.07\%$ is very small and does not depend on temperature, which is consistent with the nonmagnetic state below $T_c = 310$ K. This small ^7K is considered to be due to the Fermi contact interaction with some staying 2*s* electron.

The observed recovery of ^{7}Li longitudinal nuclear magnetization is single exponential and the relaxation rate $1/T_1$ is well defined in the entire measured temperature range. The obtained temperature dependence of $1/T_1$ is shown in Fig. 6. $1/T_1$ is nearly constant below 100 K, which is consistent with the constant $1/T_1$ for ^{51}V, and is considered to be due to the independent fluctuation of impurity V spins. The $1/T_1$ of ^{7}Li below 100 K is $\sim$0.75 s^{-1} and that of ^{51}V is 0.11 s^{-1}. The $1/T_1$ due to the localized impurity V spin fluctuation is proportional to γ^2A^2, where γ and A are the gyromagnetic ratio and hyperfine coupling constant due to impurity V spins, respectively. The ratio of the $1/T_1$ of ^{7}Li to that of ^{51}V, $^7(1/T_1)/^{51}(1/T_1)$, is written as $^7(1/T_1)/^{51}(1/T_1) = (^7\gamma/^{51}\gamma)^2(^7A/^{51}A)^2$, where $^7\gamma$, $^{51}\gamma$, ^7A, and ^{51}A are the nuclear gyromagnetic ratios of ^{7}Li and ^{51}V, and the hyperfine coupling constants of ^{7}Li and ^{51}V due to impurity V spins, respectively. $0.75/0.11 = 6.81 = 2.19 \times (^7A/^{51}A)^2$ because $^7\gamma = 16.5466$ MHz/T and $^{51}\gamma = 11.193$ MHz/T. Thus, ^7A is estimated to be $1.76 \times {}^{51}A$. This result may indicate that the impurity V spins are situated closer to Li^+ ions than to V^{3+} ions, which is consistent with the tendency that impurity V is apt to be crystallographically intercalated between the planes.[8]

In Fig. 7, we show the Arrhenius plot of the ^{7}Li $1/T_1$ data points above 270 K by circles. In this figure, the data points of ^{51}V $1/T_1$ are also shown by squares. We determine the gap Δ to be 1900 K from the slope of the solid line in the temperature range from 270 to 310 K, which agrees with 1900 K estimated from ^{51}V $1/T_1$, as can be seen by the same slope of the dotted line.

The increase in the $1/T_1$ values above $T_c \sim 310$ K indicates the existence of spin gap[8] or Li^+ ion diffusion. The inset figure in Fig. 6 shows the temperature dependence of the full width at half maximum (FWHM) of the ^{7}Li-NMR

spectrum. This FWHM is independent of temperature in the observed temperature range, that is, the motional narrowing of the ^{7}Li-NMR spectrum does not occur. Thus, Li^+ ion diffusion is not so important for the $1/T_1$ of ^{7}Li, and the increase in $1/T_1$ above 310 K proves the existence of spin gap. The existence of spin gap is supported by the facts that the Pauli paramagnetic susceptibility χ of $LiVS_2$ is smaller than that of $LiVSe_2$, although the electronic density of states in $LiVS_2$ is higher than that in $LiVSe_2$, and that χ increases with increasing temperature above T_c in $LiVS_2$.[8] These results indicate that the Pauli paramagnetic susceptibility is suppressed because the short-range ordering of the spin singlet develops and the pseudo gap is formed. The fact that the change in the entropy of $LiVS_2$ at $T_c \sim 310$ K is about one-half as small as that of $LiVO_2$ also supports the existence of the pseudo gap.[8,13] This pseudo gap can be estimated to be 720 K from the slope of the dash-dotted line fitted to the data points between 315 and 470 K in Fig. 7.

We give some comments on the superconductivity in $LiVS_2$. A $[Pd(dim)_2]_2^-$ ion in a two-dimensional triangular lattice organic compound $EtMe_3P[Pd(dim)_2]_2$[14,15] has a lone pair of electrons and reveals a dimmer spin singlet state at low temperatures. This organic compound becomes metallic under pressure, and the superconducting phase appears below 5 K in the phase boundary between the spin singlet insulator and the metallic state. However, the superconductivity cannot be observed in $LiVS_2$ even if we suppress the spin trimer singlet insulator phase by replacing S with Se ($LiVSe_2$: simple metal), which indicates that the pseudo gap might be one of the factors that suppress the superconductivity phase.[8]

4. Conclusion

We have investigated the properties of a two-dimensional triangular lattice $LiVS_2$ in the temperature range between 4.2 and 470 K by ^{51}V and ^{7}Li-NMR measurements. The Knight shifts ^{51}K and ^7K of ^{51}V and ^{7}Li-NMR do not depend on temperature and have small positive values of 0.55 and 0.07% below the transition temperature T_c, respectively, which proves the existence of a nonmagnetic state below T_c. Both of the ^{51}V and ^{7}Li spin–lattice relaxation rates $1/T_1$ reveal the activation-type temperature dependence below T_c, providing evidence for the gap structure of the electronic state with an energy gap of 1900 K. These results agree with a trimer singlet of V^{3+} spins below T_c. Below $\sim$100 K, the $1/T_1$ values of both ^{51}V and ^{7}Li are almost constant. From these constant values, we have estimated that the hyperfine field ^7A at ^{7}Li due to impurity V spins is about twice as large as the hyperfine field ^{51}A at ^{51}V due to impurity V spins. This result may indicate that the paramagnetic impurity V spins are situated closer to Li^+ than to V^{3+}.

Above T_c, the $1/T_1$ of ^{7}Li shows again the activation-type temperature dependence. However, the FWHM of the ^{7}Li-NMR spectrum is independent of temperature, which means that motional narrowing does not occur and Li^+ ion diffusion does not contribute to ^{7}Li relaxation. We can consider that the pseudo gap has already been developed above T_c and is estimated to be 720 K from the slope of the Arrhenius plot of the $1/T_1$ of ^{7}Li above T_c. This result is consistent with the increasing behavior of susceptibility with increasing temperature above T_c and with the anomalously small change in entropy at T_c in $LiVS_2$ compared with that in $LiVO_2$.

1) K. Takada, H. Sakurai, E. Takayama-Muromachi, F. Izumi, R. A. Dilanian, and T. Sasaki: Nature **422** (2003) 53.
2) W. Rudorff and H. Becker: Z. Naturforsch. B **9** (1954) 614; K. Imai, M. Koike, H. Sawa, and H. Takei: J. Solid State Chem. **114** (1995) 184; W. Tian, M. F. Chisholm, P. G. Khalifah, R. Jin, B. C. Sales, S. E. Nagler, and D. Mandrus: Mater. Res. Bull. **39** (2004) 1319.
3) M. Onoda, T. Naka, and H. Nagasawa: J. Phys. Soc. Jpn. **60** (1991) 2550.
4) H. F. Pen, J. van den Brink, D. I. Khomskii, and G. A. Sawatzky: Phys. Rev. Lett. **78** (1997) 1323.
5) J. B. Goodenough: *Magnetism and the Chemical Bond* (Wiley, New York, 1963) p. 269.
6) J. B. Goodenough, G. Dutta, and A. Manthiram: Phys. Rev. B **43** (1991) 10170.
7) B. van Laar and D. J. W. Ijdo: J. Solid State Chem. **3** (1971) 590.
8) N. Katayama: Doctor Thesis, Department of Advanced Materials Science, University of Tokyo (2008).
9) D. W. Murphy, C. Cros, F. J. Disalvo, and J. V. Waszczak: Inorg. Chem. **16** (1977) 3027.
10) A. Narath: Phys. Rev. **162** (1967) 320.
11) J. Kikuchi, S. Kambe, H. Yasuoka, Y. Ueda, K. Tomimoto, and J. Akimitsu: J. Phys. Soc. Jpn. **60** (1991) 3620.
12) T. Tanaka, Y. Kawasaki, Y. Takagishi, Y. Ideta, Y. Kishimoto, T. Ohno, N. Katayama, M. Nohara, and H. Takagi: J. Phys. Chem. Solids **69** (2008) 3142.
13) S. Niitaka *et al.*: private communication.
14) Y. Ishii, M. Tsumura, and R. Kato: J. Phys. Soc. Jpn. **76** (2007) 033704.
15) Y. Shimizu, H. Akimoto, H. Tsuji, A. Tajima, and R. Kato: Phys. Rev. Lett. **99** (2007) 256403.